Phototaxic foraging of the archaepaddler, a hypothetical deep-sea species.

(7th March 2002)

Artificial Life 4: 157 - 181

R. J. V. Bertin[1,2] (rbertin@ccr.jussieu.fr)
W. A. van de Grind[2] (W.A.vandeGrind@bio.uu.nl)

1: Current address:
LPPA
Collège de France / C.N.R.S.
11, place Marcelin Berthelot
75005 Paris
France
fax: +33 1 44271382
2: Neuroethology group
Department of Comparative Physiology
Utrecht University
&

Helmholtz Instituut
School for Autonomous Systems Research

Padualaan 8
3584 CH Utrecht
the Netherlands
fax: +31 30 2542219/2532837

Phototaxic foraging of the archaepaddler

Abstract

An autonomous agent (animat, hypothetical animal), called the (archae) paddler, is simulated in sufficient detail to regard its simulated aquatic locomotion (paddling) as physically possible. The paddler is supposed to be a model of an animal that might exist, although it is perfectly possible to view it as a model of a robot that might be built. The agent is assumed to navigate in a simulated deep-sea environment, where it hunts autoluminescent prey. It uses a biologically inspired phototaxic foraging-strategy, while paddling in a layer just above the bottom. The advantage of this living space is that the navigation problem is essentially two-dimensional. Moreover, the deep-sea environment is physically simple (and hence easier to simulate): no significant currents, constant temperature, completely dark. A foraging performance metric is developed that circumvents the necessity to solve the travelling salesman problem. A parametric simulation study then quantifies the influence of habitat factors, such as the density of prey, and the body-geometry (e.g. placement, direction and directional selectivity of the eyes) on foraging success. Adequate performance proves to require a specific body-geometry adapted to the habitat characteristics. In general performance degrades smoothly for modest changes of the geometric and habitat parameters, indicating that we work in a stable region of 'design space'. The parameters have to strike a compromise between on the one hand the ability to 'fixate' an attractive target, and on the other hand to 'see' as many targets at the same time as possible. One important conclusion is that simple reflex-based navigation can be surprisingly efficient. In the second place, performance in a global task (foraging) depends strongly on local parameters like visual direction-tuning, position of the eyes and paddles, etc. Behaviour and habitat 'mould' the body, and the body-geometry strongly influences performance. The resulting platform enables further testing of foraging strategies, or vision and locomotion theories stemming either from biology or from robotics.

Keywords: hypothetical animal, 2 light experiment, phototaxic foraging, visuomotor behaviour, foraging performance, animats.

1 Introduction

> "Upon shading or switching off the light, the "dog" can be stopped immediately, but it will resume its course behind the moving light so long as the light reaches the condensing lenses in *sufficient intensity*. Indeed, it is more faithful in this respect than the proverbial ass behind the bucket of oats. To the uninitiated the performance of the pseudo dog is very uncanny indeed."

This is a quote from an article in the Electrical Experimenter of September 1915 (quoted in [19, pages 68,69]), describing the "Orientation Mechanism" built by the "well-known inventor, Mr. John Hays Hammond, Jr.". It is probably the first example of what we now call *Artificial Life*, far predating Grey Walter's description of similar machines in the 1950s. Hammond appears to have been quite aware of the possibilities of making practical use of such a navigation mechanism, since he applied it to the "Hammond Dirigible Torpedo"...

Loeb [19] was one of the first to analyse visually-guided animal navigation, the topic of this paper, in bold mechanistic terms. He rejected the century-old idea that phototropic navigation is based on the animal's feelings of 'love' or 'hate' for light. According to Loeb the symmetry-plane of the animal's body is the basic orientation-reference. A frontal sensor on one side of this plane could innervate a caudal motor appliance on the opposite side of the symmetry-plane, leading to an automatic orientation of the symmetry-plane so as to contain the light source. These considerations lead quite naturally to the question how an animal would orient in the presence of two-lights. If the two lights are placed at equal distances from the symmetry-plane on a line perpendicular to that plane one has the equivalent of the donkey's dilemma between two sheafs of hay. Kühn [17] and Fraenkel and Gunn [12] modified and expanded on Loeb's ideas and radically changed the terminology (e.g. Loeb's tropism is now called a taxis). Countless animal species were subjected to the two-light experiment [19, 17, 12, 22] and it therefore seems like a natural point of departure for a study on visually-guided navigation, such as ours. Therefore we developed a bilaterally symmetric class of hypothetical animals, the paddlers, with two eyes in the head region and two paddles in the tail-region, placed symmetrically relative to the midsaggital plane, which is Loeb's symmetry-plane. To keep things simple and yet 'natural' we assume that these animals live in the deep-sea (no turbulence, no background-light, constant temperature, etcetera) and feed on another hypothetical species, glowballs. Of course glowballs are autoluminescent, so they look like swimming light bulbs. More details are given later on.

The two-light experiment is of interest since it has been carried out on many animals and since it gives perhaps the simplest and most basic information on orientation and navigation in an environment with more than one target. However, one might wonder why animals would bother to move towards or away from light sources in the first place. Our paddlers have a clear and vital reason: to fill their stomach and survive. In such a situation it would be reasonable to expect that evolution leads to more sophisticated navigational strategies and better methods of choosing the next target in a larger collection of food items. We were therefore interested in two basic questions. First, if a very simple paddler, almost built to the specifications of Loeb, behaves as expected in the two-light (two-glowball) situation, how does it behave in a living-space with many glowballs? Second, how can or should the inevitable shortcomings be remedied? In other words, what are the simplest conceivable improvements on Loeb's scheme. To study these questions quantitatively one has to solve a number of auxiliary problems. First, how do we quantify foraging success? Second, what is the influence of body-geometry on foraging success?

It would be nice to simulate a complete evolution of the paddlers and thus answer the second main question and the second auxiliary question empirically. One would merely need to specify the environment, a simple ancestral species, a selection criterion and then wait and see what evolves. However, such an approach is still too complex at present since it requires a specification of the relation between genetic information and to the resulting neural networks and body-geometry. Therefore we resorted to tinkering in the sense of the evolutionary process [11]. With our criterion of foraging-success, as specified later on, we carried out a parametric study of paddlers. This enabled us to fix all parameters so as to optimise foraging success. Further improvement then requires some innovation. The boundary conditions for choosing an innovation are: 1) that it is known to exist in some animal and 2) that it seems like a small step relative to the existing design. For example, after developing the simple archaepaddler L (L for Loeb) and studying its behaviour in a multi-target environment like ethologists study real animals, we feel the

animal needs some mechanism for "course-stabilisation". Two well-known principles were implemented to achieve that goal, namely directional weighting (tuning) of the visual receptor-layer and giving binocular information additional influence to emphasise straight-ahead relative to course-changes. These innovations lead to a new species, the archaepaddler B, which proves to perform quite well in complex multi-target environments. It is in turn the starting point for the development of a more sophisticated navigator described elsewhere [4], a paddler that can handle a wide range of background light intensities and both positive and negative contrast of the target. These adaptations are necessitated by migration to shallower water.

Phototaxis is the "visual version" of *tropotaxis*, a kind of autonomous closed-loop navigation in which sensory excitation in the nervous system is kept (left-right) symmetric by motor actions governed by the same sensory information ([17], following [19]). This principle is nicely illustrated in [5], but also in [24, 25]. Tropotaxis of chemical nature (*chemotaxis*) is demonstrated in [1]. We will use the term *phototaxic navigation* for visually-guided tropotaxis based on a bi-sensor system (two eyes) with a directional sensitivity-tuning of each of the two sensors (eyes). A Gaussian weighting function, gives each eye a specific direction of maximal light-sensitivity (the line of sight) flanked by regions in which sensitivity declines smoothly, as it does in many bi-sensor systems [22]. If the width-parameter of this weighting-function is made very large one has the Loeb system, without visual direction tuning. Therefore we add this 'innovation' of visual direction-tuning right from the start and regard the archaepaddler L as a limiting case of the more general archaepaddler B. There are several levels of detail in which acting animals can be modelled. In general, more complex behaviours are best modelled at a higher, more schematic level of description (e.g. [8]), with more detailed, biophysical aspects (such as those of locomotion) approximated or taken for granted. However, since the animal's actions are its interactions with its environment, they directly influence its sensory input. Therefore studies in which sensorimotor behaviour is modelled at a more detailed level of description (e.g. [7, 10, 9]), and also studies aiming at realistic animation of behaviour (e.g. [23]) do explicitly model these physical aspects. Here, we simulate the physical processes of locomotion in sufficient detail to view it as representative of locomotion in real animals. This leads to the following nontrivial result. Habitat, foraging-strategy and body-form have a strong influence on each other: The environment-animal interactions shape the body and the animal's behaviour, like an artist would a piece of clay!

2 The archaepaddler

Fig. 1 depicts the archaepaddler (or simply *paddler*, for the purposes of this paper), a hypothetical animal with a circular body of radius R.

FIGURE 1 ABOUT HERE.

Apart from a pair of eyes, a mouth, a "catch region", paddles for locomotion, and a pair of pectoral fins (*pectfins*) to help in course stabilisation, there is a simple nervous system (NS), to be described below. The first problem we now face is to choose a body-structure for the paddlers that is compatible with Loeb's ideas, but at the same time specifies all the parameters. Where do we place the eyes and paddles, at what angle relative to the plane of symmetry, how wide do we make the visual field of the eyes and in what direction should the visual weighting be maximal (the direction of the line of sight)? Since all these factors are under survival pressure, we cannot fix them a priori. The only option left is to introduce a whole list of structural parameters and do a parametric study. The eyes are positioned at an angle α relative to the rostro-caudal body-axis and have a visual field of φ degrees centred on their eye axis, which makes an angle of β degrees with the rostro-caudal axis. For the purposes of this paper the exact anatomy of the eyes (lens eye or compound eye) does not matter, provided it has some directional selectivity.

It is known that light of the dominant autoluminescent wavelengths (which humans would call *blue-green*) can be seen from a maximum distance of 10-16 m in the deep sea [18]. This "effective visual horizon" is the result of absorption and scattering by the water and the particles suspended therein. As an approximation, to be approved below, we therefore introduce an explicit visual-horizon parameter in the simulations, called D (maximum visual distance).

The retina consists of $N = 80$ equally-spaced identical photoreceptors. To give the eyes a best visual direction the contributions of these receptors to the eye's response are weighted as indicated in Fig. 2. The retinal weighting function (RWF) has a Gaussian shape with halfwidth σ and an optimum direction called the visual axis. The visual axis makes an angle of ε degrees with the eye axis (Fig. 1) in such a way that binocular vision can be favoured over monocular vision (see below). The visual axes cross in the "fixation point"[1] F on the paddler's longitudinal body axis (see figure 1); the distance from the centre of the eye to F is called the fixation distance D_f. A fixation distance of $\mathrm{D}_f = \infty$ thus denotes a visual axis parallel to the paddler's longitudinal axis ($\varepsilon = \beta$).

FIGURE 2 ABOUT HERE.

The eye needs separate photoreceptors (or receptive fields) in order to resolve separate targets, but in the archaepaddler information about targets is pooled early in the visual system. Each eye's output is a visual-direction-weighted estimate of the amount of light reaching the eye from the corresponding part of the world. More precisely, it is the weighted sum of all photoreceptor outputs, divided by the number of active receptors. This principle of directional tuning of the bi-sensors can, depending on the choice of parameter values, facilitate course stabilisation with a preference for straight-ahead or small yaw angles. In fact, directional sensitivity improves performance (the reliability of finding a source) even in one-sensor organisms [16]. The influence of the weighting function can be seen intuitively from Fig. 2 by considering a small glowball *G1* close to the optimal direction and a larger glowball *G2* in a more peripheral direction. Thanks to the weighting *G1* gives a stronger response. Thus if *G1* is seen by one eye and *G2* by the other eye the smaller course change necessary to catch *G1* will win out over the larger course change to catch *G2*, even though *G2* is bigger (or closer). The parameters of this weighting function allow us to play with this type of preference. Obviously if the halfwidth is large, directional tuning disappears, and *G2* in the example might win and the animal might more easily change course to catch bigger or closer prey at higher eccentricities. The choice of this parameter is one of the differences between the L and B versions of the archaepaddler. The other difference is that the B paddler has an additional parameter ϖ ($\varpi = 0$ in the archaepaddler L), the binocular facilitation parameter which also plays a role in course stabilisation (see later).

Summarising, the eye-position and eye axis (parameters α and β) determine which portion of the outside world is sampled. The visual axis (ε) and RWF halfwidth (σ) determine how it is sampled, i.e. how the sensitivity is distributed over the sampling area.

The nervous system. The nervous system (NS: figure 3) converts the eye-responses into the appropriate swim commands. It is a feedforward network with analog components (neurones). Communication between the neurones is represented by real numbers (range [0,100]) which stand for spike frequencies. There are three types of synapses: excitatory (addition), inhibitory (subtraction) and shunting inhibition. Shunting inhibition is implemented by dividing input x by $(i + 1)$, where i is the inhibitory signal.

FIGURE 3 ABOUT HERE.

The NS is inspired partly on specific, real biological systems (e.g. the paddle controllers, see below), partly on general principles found throughout the animal kingdom. It has three distinct centres. The *normalising centre* remaps the eye-responses onto a constant interval by dividing each eye-response by the sum of both eye-responses. Responses from the binocular regions of the eyes are pooled and receive additional (ϖ) weight in the B paddler, but not in the Loeb version. The *visuomotor centre* maps the visual signals onto motor command and control. Two leaky integrators (modelled as first order lowpass filters with timeconstant τ) filter out fast fluctuations and serve as a short-term memory for direction of movement, another course stabilisation mechanism. A mutual inhibition between the two leaky integrators (suppressed in the presence of visual information) amplifies the last manoeuvre (started before visual

[1] Just like we use the term "fovea" (the direction of maximal sensitivity) as an analogue to its standard meaning as "the retinal region of maximal resolution", "fixation" in this context does not imply that the paddler is actually capable of fixating a given point! Response to a target moving along the paddler's longitudinal axis is strongest at the fixation point.

information ceased) by silencing the weaker of the two leaky integrators. In the absence of visual information, the paddler's movements are determined by a *wander controller*. This is a network of mutually inhibiting neurones with stochastic spontaneous activity. It generates swimming bouts of random speed and direction. During visually-guided behaviour it is inhibited by a neurone integrating the responses of both eyes. The same neurone gates the mutual inhibition between the two leaky integrators. A *motor centre* uses the signals from the visuomotor centre to create swim commands.

Locomotion and its control. The paddles are stiff appendages positioned as indicated in figure 1. Movement of the paddles is controlled by two *paddle controller* networks. These are oscillatory networks that convert a tonic motor command (the *central swim command*) into the alternating muscle commands that drive the antagonistic levator (up) and depressor (down) paddle muscles [26, 27]. A feedback control loop compares the actual force excerted on the paddle with the required force, and sets the gain of the muscle innervation accordingly.

A speed control system regulates the paddler's actual swimming speed. This system derives the required speed from the central swim commands, and compares it with the actual speed, setting the gain to the paddle controllers accordingly. If the actual speed is too large, the pectfins are tilted accordingly in order to brake. Actual speed is measured from deflection (amount and direction) of a contralateral pair of hair-receptors caused by the water flow around the body. The direction of movement is labelled-line encoded: rostro-caudal and caudo-rostral water-flow activate different channels. Required speed is similarly represented in swim direction/speed vectors. On each side of the paddler, the four possible, qualitatively different combinations of required and actual speed are used to determine a left/right set of four *elementary gain factors*. Contralateral combinations of those elementary gain factors are then used to determine the gains to the paddle controllers and possibly the brake commands. The speed control system compensates for inertia, and also for the slower acceleration at low thrust (see below). Especially the paddler's turnability benefits from this. It also enables the paddler to swim forward by using its tail fin (much like a gondolier rows his gondola) when the paddles can only generate rotational thrust (as happens when the generated thrust is parallel to the body).

A more detailed description of the locomotor system and a motivation of the design will be given elsewhere (see also [3]). For the experiments described in this paper, a simplified *linear* paddle controller was used. This controller linearly maps the central swim command onto a paddling force (thrust). This linear mapping is a good approximation of the mapping performed by the more complex oscillatory paddle controller.

A summary of the physics of the paddler's locomotion is given in Appendix A. Although some aspects of this design of the locomotor system might seem arbitrary at first sight, there really is not much freedom in designing such a system given the physical constraints and the goals of cruise control.

3 Methods

A. The simulated environment Three paddlers were allowed to roam an unlimited patch of deep sea. An open, rectangular section of this space served as a foraging environment: in this foraging space, a number of glowballs was distributed. At fixed intervals, eaten glowballs were replaced (i.e. made visible to all paddlers) at their initial position, in order to prevent depletion.

An experiment consists of an observation of the 3 identical paddlers over a certain time, during which data are collected, averaged over the 3 paddlers and stored at the end of the observation-time. Paddlers venturing too far from (i.e. loosing visual contact with) the foraging space are replaced at a random position within the foraging space. This procedure was repeated for each value out of a fixed range of the parameter-of-interest. During these experiments, there is no interaction or competition between the different paddlers: they don't exist for each other, and a glowball eaten by one remains visible and edible for the other two. Thus we collect data on 3 independent, identical paddlers in the same environment and with the same settings in parallel, because it is fast and convenient in our setup. It has no principled significance.

B. Performance index. It can be expected that classical, positive phototaxis is an adequate strategy for foraging in a deep-sea environment. The actual foraging performance depends on the "tuning" of the animal's geometrical and physiological *parameters*. The following experiments address the influence of several of these parameters on the paddler's overall performance, as quantified in terms of a performance index $\wp$. The value of this index mirrors the "fitness" of the corresponding individuals.

A useful way of determining a performance index is by dividing the distance covered by a paddler in a given period (D_t), by the number (G_e) of glowballs eaten during that period. To normalise for different glowball densities, the number of glowballs eaten is multiplied by the average distance ($\langle \mathrm{D}_m \rangle$) from a given glowball to its nearest neighbour:

$$\wp = \frac{\mathrm{G}_e \cdot \langle \mathrm{D}_m \rangle}{\mathrm{D}_t} \tag{1}$$

The average distance between nearest neighbours $\langle \mathrm{D}_m \rangle$ is calculated by an algorithm that starts with the glowball nearest to the centre of the foraging environment; determines the distance to its nearest neighbour; finds the nearest neighbour of that glowball, etc. Hence the distances measured reflect the minimal distance to the nearest *uneaten* glowball. As a result, some distances may be quite large! The $\wp$ index approaches 1 for the case when a paddler repeatedly takes the direct route from one glowball to its nearest neighbour. When no further information on glowballs or routing is available, this is the optimal foraging strategy [21]. Lower values indicate lesser performance; significantly larger values are an indication that the index has become invalid, probably due to an overestimated $\langle \mathrm{D}_m \rangle$ value

C. Simulation Methods. Experiments were carried out using a proprietary simulation package written in ANSI C, and run on HP 9000/730 and Apollo DN10000 computers. The simulated two-light experiments on the archaepaddlers L and B are described below, in the Results section. In all other experiments, B-type paddlers were "released " in a foraging space of 150 length-units square, and observed for 4000 or 5000 steps (time-units), each with a resolution of 0.033, i.e. 30 clock-ticks per time-unit), during which data were collected. Into this foraging space a number (G) of glowballs between 64 and 625 were uniformly distributed, eaten glowballs were replaced every 500 or 1000 steps. The glowballs had a radius of 0.5 ± 0.144 length-units (uniform distribution; *large individuals*). In some experiments, *small individuals* of radius 0.02 ± 0.00289 (also uniform) were used. Glowball luminance was set at 50 ± 0.279 (uniform). The paddlers had a radius of 2 length-units and a mass of 500 mass-units. In the course of our simulation studies we systematically explored the multi dimensional parameter-space of the archaepaddlers. Except for pathological cases (like eyes and paddles at the same position), most parameter-combinations gave some foraging success, but a reasonable and reasonably flat optimum was found for the parameter values in Table 1. It would not be instructive nor interesting to discuss all of these studies here. In the experiments presented below we therefore concentrate on the more interesting parameters of the paddlers and their environment.

parameter	*value*	*comment*
α	90°	eye-position; varied in experiment **2**
β	20°	eye-axis; varied in experiment **2**
φ	140°	width of the eyes' field of view
σ	15°	halfwidth of the RWF (B-type paddlers) varied in experiment **3**
D_f	11.5	fixation distance in length units varied in experiment **4**
ε	-30.0154°	the visual axis: the value listed corresponds to $\mathrm{D}_f = 11.5$
D	10	visual horizon in length units
κ	45°	angular width of the mouth length of the mouth: 1.46 length units
δ	130°	paddle-position
ρ	-20°	paddle-rotation
ϖ	0.5	binocular weight (B-type paddlers)
scotopic threshold	10^{-10}	lowest luminance level at which the visual system works

Table 1: Default parameters of the archaepaddlers.

Experiments were done in two types of environment. We will first discuss the experiments performed in an environment with absolutely clear water (without any absorption of light), and in which an *ad hoc*, relatively "close", hard visual horizon (D) is imposed. Then, we will discuss the effects of a more realistic environment where a substantial amount of light is absorbed; where glowballs are less bright, the paddlers' thresholds higher. In these experiments, the visual horizon is a result of available light, absorption and internal thresholds; these are tuned such that the paddler can see glowballs of average brightness up to a distance $\approx \mathrm{D}$.

4 Experiments and results

Experiment 1: The two-light experiment. To asses to what extent our hypothetical animal's navigation might be representative of a simple, real animal's behaviour, we performed some two-light experiments [12]. In the environment just described, two identical, "large" glowballs were placed at a distance of 30 length units from each other. A single paddler was repeatedly placed approximately on the line through the midpoint of, and perpendicular to the line segment connecting the two glowballs. The initial position was slightly varied across trials. The paths taken by the paddler were recorded and are shown in figure 4. For comparison, figure 4a shows the paths for *Corophium longicorne* (figure 73, op. cit.). Figure 4c shows the paths taken by a B-type paddler as described above. Figure 4b presents the paths taken by an L-type paddler with the same parameters (but of course without directional selectivity ($\sigma = \infty$) and no extra binocular weighting). The B- and L-type paddlers were released from the same starting positions.

FIGURE 4 ABOUT HERE.

There is a striking difference between the paths taken by the L-type (fig. 4b) and the paths taken by the B-type (fig. 4c) paddlers. The L-type paddler behaves much like the the real animal of figure 4a. It can clearly be seen that the RWF and the extra binocular weighting significantly increase the paddler's decisiveness (fig. 4c). From these data, one can conclude that *Corophium l.* has few or no mechanisms to increase its directional selectivity. The L-type paddler is a satisfactory model. Some more observations can be made. Each point of the traces in figures 4b & 4c represents the centre of the paddler's body; the switch to searching behaviour after having eaten a glowball thus seems to occur at some distance from the glowball. The amplified continuation of the last manoeuvre is noticeable. Here the distance between the 2 glowballs is larger than D (but smaller than $2\mathrm{D}$), which explains why only one target was chosen per experiment. Lastly, even when the paddler is initially trapped in a donkey's dilemma (i.e. when it receives equal stimulation on the left and right), its searching mechanism causes it to choose one

glowball (at random) after having passed both. As the donkey's dilemma is an unstable equilibrium, it is most unlikely that a paddler or indeed a real animal will ever get into one during their "real life".

Experiment 2: The influence of eye-position parameters α and β. In this experiment, we study the influence of eye-position on foraging performance. To this end, the eye's position on the body was systematically varied from fully frontal to fully lateral (i.e. $\alpha \in [0°, 90°]$). The direction of the eye axis was varied independently, such that the eyes were either looking both outward, or both inward ("squint"), and a number of directions in between (i.e. $\beta \in [-90°, 90°]$). The other parameters were as listed under *Methods*, except that the eyes' visual axis is along the eye axis for fully frontal eyes ($\varepsilon = 0°$ when $\alpha = 0°$; in this case we define $\mathrm{D}_f = 0$). The results are shown in figures 5 for a low glowball density and in figure 6 for a high glowball density, in both cases for populations of large glowballs.

FIGURE 5 ABOUT HERE.

FIGURE 6 ABOUT HERE.

In both figures, it can be clearly seen that there is a very broad range of eye-position/eye-axis combinations that allow adequate foraging. Contrary to what might be expected intuitively, this is especially true for *low* glowball densities (fig. 5). At high glowball densities (fig. 6), eye-position/eye-axis tuning is sharper, in the sense that some combinations give rise to highly inferior performance. For most "sub-optimal" combinations (generally $16 \leq \beta \leq 64$), performance is better, possible due to the increased probability in high densities of blindly stumbling upon a glowball. Optimal performance is the same in both densities. For low glowball densities of $\mathrm{G} = 121$, the average distance between nearest neighbours has at least the value of the visual horizon ($\langle \mathrm{D}_m \rangle \geq \mathrm{D}$), meaning that there is on average just one glowball visible at any given moment. For higher densities, more and more glowballs become visible at any moment. As a result, equalising the luminance-responses in both eyes doesn't necessarily lead the paddler to a glowball. It may even cause it to take a middle-course between two equally attractive glowballs and thus miss both. Of course, such indecisiveness reduces the foraging effectiveness; thus the eye-position/eye-axis tuning becomes sharper.

In the case of extreme squinting (strongly negative values of β), and or fully frontal, squinting eyes ($\alpha = 0°, \beta < 0°$), performance decreases dramatically. This is the result of *negative phototaxis* because now each eye is looking at the wrong (contralateral instead of ipsilateral) half of the world. This explanation is supported by the fact that for eyes placed in this manner, the paddlers have on average smaller eye-responses (i.e. they shun light, which minimises retinal illumination) than paddlers with normal positive phototaxis.

When there are many glowballs, frontally placed, outward looking eyes (low α and moderately large, positive β respectively) cause a drop in performance. The geometry of the overall visual field of this kind of eyes is such that we now have two small but sensitive regions just outside of the binocular region in which phototaxis is negative. In the rest of the overall visual field (the combined visual fields of both eyes; surrounding the negatively phototaxic parts), phototaxis is positive. In the middle of a glowball population, behaviour is quite normal. However, a dense population contained within a restricted area possesses relatively distinct borders. Once a paddler with this placement of the eyes reaches such a border, it will in many cases start following it, clearly no longer foraging. This edge-following behaviour results from the fact that the glowball population as seen by the outer, positively phototaxic part of a visual field will cause the paddler to turn towards the population. Due to the high density, chances are very high that the small negatively phototaxic part of the eye's visual field will receive stimulation, which, given its high sensitivity, causes the paddler to respond vigorously. As a result, the paddler turns away again, loosing the negative stimulation.

At medium to low glowball concentrations, chances are low to very low that the negatively phototaxic part of the visual field receives much stimulation because on average the distance between glowballs is larger than the visual horizon ($\langle \mathrm{D}_m \rangle > \mathrm{D}$). Also, such a population does not show distinct borders.

The results of figures 5 and 6 show that the default values for eye-position and eye axis ($\alpha = 90°$ and $\beta = 20°$ respectively; as listed in Table 1) are compatible with a high performance. The orientation of the eye axis (β) is the parameter most dramatically affecting foraging performance in these environments.

Experiment 3: The retinal weighting function. In the third set of experiments, we address the influence of the halfwidth σ of the eye's retinal weighting factor (RWF) on the foraging performance. It can be expected that intermediate values give the best performance: they allow for selectivity (especially at high glowball densities), while not sacrificing too much of the visual field. Figures 7 and 8 show the results of two simulations: one with large glowballs, and one with small glowballs, in both cases for 4 different target densities from low (64) to high (625).

FIGURE 7 ABOUT HERE.

FIGURE 8 ABOUT HERE.

Intermediate halfwidths indeed give the best performance, but only for higher glowball densities, and most clearly for large glowballs. Roughly speaking, the halfwidth should lie between 10° and 50°, that is $3 \cdot \sigma < \varphi$, meaning that the Gaussian distribution is narrower than the visual field. When there are only few glowballs, a larger halfwidth (meaning a larger *functional* visual field) is no longer a disadvantage: there are simply no glowballs to be distracted by.

In populations with small glowballs, the overall picture remains the same, except that performance doesn't degrade that much for higher halfwidths. Since small glowballs are easier to miss, a larger functional visual field increases foraging success, and the best performance occurs at somewhat higher halfwidths (except again for high densities — $\mathrm{G} = 625$).

Performance is best at low-to-intermediate glowball densities, where the average number of visible glowballs is approximately 1. This is of course due to the fact that the present simple positive phototaxis strategy doesn 't allow for selective attention. When more than one glowball is visible at a given moment, the paddler tends to head towards the "centre of gravity " of the luminance distribution that these glowballs project on its retinas. Under circumstances, it might then miss all of the targets.

Experiment 4: The influence of the angular distance between eye axis and visual axis. This experiment addresses the influence of the direction of maximal sensitivity of the retinal weighting function, the visual axis, as expressed in terms of the fixation distance D_f.

Figures 9 and 10 show results for moderately low ($\mathrm{G} = 121$) and high ($\mathrm{G} = 625$) glowball densities, and a number of eye-positions (α). To get a stronger dependence of performance on the fixation distance, the halfwidth of the retinal weighting function has been reduced to $\sigma = 5°$ in these experiments.

FIGURE 9 ABOUT HERE.

FIGURE 10 ABOUT HERE.

The results show first of all that the fixation distance should not be (much) smaller than the visual horizon. Again, this is a result of negative phototaxis resulting from eyes that are most sensitive in directions in which the contralateral eye should have a stronger response. An additional factor at small fixation distances is that an increasing part of the visual field becomes unreceptive to visual stimulation. In other words, the paddler becomes increasingly visually handicapped (one might interpret it as tunnel vision).

It can also be seen that for fixation distances above 10 length-units, performance remains more or less optimal. There is some indication that performance is best for fixation distances between 10 and 15 length-units, i.e. with the binocular point of highest sensitivity at or just beyond the visual horizon (D). This also holds for visual horizons $\mathrm{D} \in \{5, 25, 50\}$ length-units, indicating that the direction of optimal sensitivity is closely coupled to the visual horizon (a property of the medium).

Experiment 5: The influence of a more realistic, absorbing, medium. The fact that the optimal visual axis is related to the visual horizon, raises the question what it would be for a more realistic description of absorption in the medium.

We therefore repeated the above experiments after including a model of light-absorption by water. Luminance L as a function of distance (d) to the source (with luminance L_0) in a medium with an absorption-coefficient Ω, is given by (see e.g. [20]):

$$L[d] = L_0 \cdot e^{-d \cdot \Omega} \tag{2}$$

The threshold for switching to searching behaviour and the scotopic threshold were set to a higher value (10^{-5}). Glowball luminance was reduced to $5 \times 10^{-4} \pm 3.14 \times 10^{-5}$. Absorption by the medium was chosen in such a way that a glowball of average luminance remained visible up to a distance of 25 units (thus $\Omega \approx 0.156$; the visual horizon is now no longer a "hard" boundary).

A striking effect of such a strong absorption is a phenomenon that might be described as "binocular absorption parallax". Due to unequal target-to-eye distances, the two eyes can receive different illumination from a single target. This can lead to zig-zag locomotion for body-sizes that are large in relation to the visual horizon as set by absorption.

In general, however, the results were qualitatively similar to the results described above. Absorption by the medium acts as a filter comparable to the retinal weighting function. Therefore, a broader halfwidth ($\sigma \approx 35°$) is favoured (this increases the probability of detecting a glowball). The optimal fixation distance (for $\sigma = 5°$) is slightly larger than it would be with a "hard" visual horizon at the same distance: $\mathrm{D}_f \approx 36$. This reflects the fact that the "absorption horizon" is not a clear-defined border: brighter-than-average glowballs can be seen over a larger distance than less bright glowballs. No effect was found on the optimal eye-position parameters.

5 Discussion

5.1 Phototaxic navigation: a robust strategy.

Simple forms of phototaxic foraging, based on Loeb's proposals and checked for many species in two-light experiments also suffice — i. e. can be adaptive — in an environment with many targets. Two innovations improving course stability were added: a retinal weighting function which gives directional selectivity, and extra weighting of binocularly visible targets which serves as a crude fixation mechanism. We then performed a number of simulations to study how habitat parameters and body-geometry influence performance. The simulation experiments indicate that a compromise should be found between on the one hand the ability to detect and react to as many targets as possible and on the other hand the ability to concentrate on as few targets as possible. The Gaussian directional selectivity shows this clearly (see e.g. figure 7): when the selectivity curve is too narrow, performance is bad since only the nearest or brightest glowballs are seen; when it is too wide, performance is bad because the paddler can 't decide which of all visible glowballs to select. Using a substantially different approach, Cliff and Bullock [6], reported similar results.

Within these constraints, a surprisingly large freedom of parameter choice exists. Adequate foraging performance results for many, even intuitively disadvantageous parameter settings. This might be taken to indicate that our quantification of performance in terms of the index $\wp$ is unsatisfactory. We think this is unlikely because it compares performance against the strategy "go to the nearest visible neighbour", which is the optimal strategy in this paradigm [21][2]. It therefore appears more likely that a wide range of parameter variation is acceptable in an "easy" environment that does not pose strict requirements (on foraging strategies). In other words, this finding suggests that the overall design of this type of autonomous agent is very robust.

Being able to detect as many glowballs as possible can be accomplished by having the eyes as widely apart as possible, and "looking" slightly outward (a larger visual field). Indeed we do find a slight performance increase for such a geometry. Eyes looking too much inward and set too close together can cause parts of the visual field to become negatively phototaxic: in those regions the (squinting) eyes respond better to contralateral then to ipsilateral targets. This can result in a substantial performance decrease. Such a geometry can even result in a visuomotor system that follows the edges of (dense)

[2] And indeed performance indices measuring energy expenditure give similar results.

glowball populations in an endless loop of attraction/repulsion by glowball light. An extreme convergent squint decreases the paddler's fitness.

From these results we derive two predictions for real animals using the phototaxic foraging strategy. In the first place, we predict that the within-species variation of the eye position can be quite substantial. But, in the second place, we predict that squinting will be virtually absent in the populations. We are not aware of quantitative studies in real animals that allow us to test these predictions at present. On the whole, there is an amazing paucity of statistical data on the geometrical parameters of animal-bodies. Our study shows that such data would be important in connection with theories on, or models of navigation systems.

Our earlier experiments on extremely light paddlers (that do not need a speed control system since acceleration and deceleration are almost instantaneous) favoured intermediate eye-positions, that resulted in more stable locomotion (less "wobbly"). Locomotion that is too wavery tends to cause more "glowball misses", thus impairing foraging performance. The (more biologically plausible) heavier paddlers discussed in this paper do need the speed control system; due to the larger inertia, locomotion then even remains stable for extreme eye-positions. This leads to the prediction that there is a positive correlation between mass and the presence and quality of speed control.

5.2 The influence of the eyes' directional tuning.

A similar reasoning can be applied to the directional selectivity as specified by the retinal weighting factor (RWF). Too narrow an RWF will reduce a (large) visual field to a substantially smaller functional visual field. Too wide an RWF will lead to unstable locomotion: peripheral glowballs can then cause the paddler to wander away from a close glowball straight-ahead. Simulations in which the width of the RWF was varied support this: performance is best for an intermediate width. In low-density glowball populations there is less risk for distraction by peripheral glowballs: for these densities, performance does not degrade as much for wider RWFs as it does for higher densities.

The direction of the maximal sensitivity of the RWF (in other words, the fixation distance $\mathbb{D}_f$) also has a substantial influence; performance is best when $\mathbb{D}_f \approx \mathbb{D}$. More inward tuning ($\mathbb{D}_f < \mathbb{D}$) causes parts of the visual field to become negatively phototaxic. More outward tuning ($\mathbb{D}_f > \mathbb{D}$) places too much sensitivity in the periphery. In addition, differences in eye-response to different targets just in front can become too large. All these effects cause unstable locomotion (or too little "concentration"). The constraints on the compromise between directional selectivity and "fixation capability" increase with increasing glowball densities; all studied paddlers have difficulties when several glowballs are visible at any given moment. This problem can only be solved by the evolution of a selection mechanism that allows a paddler to fixate (concentrate) on a single glowball. An interesting challenge that might lead to a more advanced species of paddler.

5.3 Advantages of the tinkering method.

The present model has been specified in such a way that it is easy to evolve. In principle, this could be done using genetic algorithms [14] or classifier systems [15] which simulate evolution from randomly disturbed inheritance of parameters and a competition for food among members of the generations that coexist. However, this is a very time-consuming technique, both computationally and from an implementation point of view. We would have to solve the problem how to encode a nervous system in a genome (e.g. [2, 7]), which is not directly relevant to our interests in the adaptive radiation of navigational strategies. Even if such an approach were far less problematic, our method of "manual evolution", i.e. to "design" animal classes and refine them with parametric simulations and by adding, changing or deleting connections, neurones, etc, might still be preferable in many cases. It provides a deeper insight in the influence and interactions of the various parameters of the animal-habitat coupling mechanisms. In short, tinkering [11] at the organismic and network level can be a powerful method of studying the possible adaptations (design space) of hypothetical and real animals in quantitative detail. This approach is not inferior to evolutionary simulations if it is constrained by biological knowledge and combined with parametric simulations which can show us what the stable and optimal regions are in design space.

5.4 Future work.

The paddlers provide a convenient platform to develop and test more complex foraging strategies and/or to test hypotheses about visual processing or motor control in real animals. Some examples of future research opportunities, directly inspired on our current findings are:

— To simulate neural networks that compare direction, distance or size of all the glowballs in view, and use this "knowledge" to optimise the choice of the next target.

— To introduce map-like memories of regional visual analyses so that the paddler can plan a path before it "hits the road".

— As our insight into the physics of locomotion deepens, to improve on the present simple specification, and test more sophisticated theories of neuronal control of locomotion.

We have already reported on mechanisms for dark/light adaptation in the diurnal paddler, a close relative of the B-type archaepaddler [4]. Research is currently under way to evolve a motion detection system from the dark/light adaptive system, and to use the new motion parallax information to improve visual analysis of relative distances and/or relative motion of external objects.

Appendix A: Locomotion

An overview of the geometry of locomotion is given in figure 11. When $\rho \neq 0°$ the thrust-vector generated by both paddles has a rotational component and a translational component. Since the rotational component of the thrust-vector is generally small with respect to the translational component, and the paddles themselves generate only a very small drag, a stiff tail fin has evolved to increase rotational drag. Due to this tail, drag-induced torque keeps the paddler's long axis aligned with the direction of movement.

FIGURE 11 ABOUT HERE.

We assume that the paddler can be considered a solid body moving in a homogenous, laminar medium. Thus simple mechanics (*Stokes law*; see e.g. [28]) tells us that its translational speed (v) can be approximated using the following equations:

$$v^{\bullet} = \frac{T_{trans} - 0.5 \cdot D \cdot f_d \cdot v^2}{M} \tag{3}$$

T_{trans}, the resultant translational thrust, can be expressed as a constant ($f_s = 1$; the speedfactor) times the translational component of the thrust-vector (F_{trans}):

$$T_{trans} = f_s \cdot F_{trans} \tag{4}$$

The resultant frontal drag-factor, f_d, depends on the frontal drag-coefficient (C_w) of the paddler's body, and the current angle of movement (Δ):

$$f_d = C_w \cdot \left|\sin[\Delta]\right| + C_w \cdot \left|\cos[\Delta]\right| \tag{5}$$

The angular speed (ω) can be approximated with:

$$\omega^{\bullet} = \frac{T_{rot} - 0.5 \cdot D \cdot C_{rw} \cdot \omega^2}{M} \tag{6}$$

T_{rot}, the resultant rotational thrust, depends on the rotational component of the thrust-vector (F_{rot}) and the current speed and direction of movement:

$$T_{rot} = f_s \cdot \left(F_{rot} + C_w \cdot \left(v \cdot \sin[\Delta]\right)^2\right) \tag{7}$$

with:

$v^{\bullet}$ ($\omega^{\bullet}$) the current (angular) acceleration.

M the paddler's mass. We take $M = 500$.

D the density of the medium. We take $D = 1$.

The area of the tail fin is expressed in terms of the radius R of the paddler 's body. The tail fin can be divided into two sections: one "above" the body and one extending behind the body. The part above the body has length R and height $\frac{1}{4} \cdot R$, which is half the body height. The part extending beyond the body has length $\frac{1}{2} \cdot R$ and height $\frac{3}{4} \cdot R$. Paddle-induced drag is neglected, which gives us a radial drag-coefficient $C_{rw} = \frac{65}{96} R^4$.

Acknowledgements

The research presented in this paper was part of a PhD project supported by a grant from the Foundation for Biophysics (presently Foundation for the Life Sciences) of the Netherlands Organisation for the Advancement of Scientific Research (NWO).

References

[1] **Beer R.D. (1990)** *Intelligence as Adaptive Behaviour - An Experiment in Computational Neuroethology*. Boston, Academic Press 1990

[2] **Beer R.D. and Gallagher J.C. (1992)** *Evolving Dynamical Neural Networks for Adaptive Behavior*. Adaptive Behavior 1 1992: 91-122

[3] **Bertin R.J.V. (1994)** *Natural smartness in Hypothetical animals-Of paddlers and glowballs*, PhD thesis, Utrecht University.

[4] **Bertin R.J.V. and van de Grind W.A. (1996)** *The influence of light/ dark adaptation and lateral inhibition on phototaxic foraging. A hypothetical-animal study.* Adaptive Behavior 2 1996: 141-167

[5] **Braitenberg V. (1984)** *Vehicles - Experiments in Synthetic Psychology*. Cambridge, MA, The MIT Press 1984

[6] **Cliff D. and Bullock S. (1993)** *Adding "Foveal Vision" to Wilson's Animat*. Adaptive Behavior 2 1993: 49-72

[7] **Cliff D., Husbands P. and Harvey I. (1993)** *Explorations in Evolutionary Robotics*. Adaptive Behavior 2 1993: 73-110

[8] **Corbacho F.J. and Arbib M.A. (1995)** *Learning to Detour*. Adaptive Behavior 4 1995: 419-468

[9] **Cruse H., Brunn D.E., Bartling Ch., Dean J., Dreifert M., Kindermann J. and Schmitz J. (1995)** *Walking: A Complex Behavior Controlled by Simple Networks*. Adaptive Behavior 4 1995: 385-418

[10] **Ekeberg O., Lansner A. and Grillner S. (1995)** *The Neural Control of Fish Swimming Studied Through Numerical Simulations*. Adaptive Behavior 4 1995: 363-384

[11] **Jacob F. (1977)** *Evolution and tinkering*. Science 196: 1161-1166

[12] **Fraenkel G.S. and Gunn D.L. (1961)** *The orientation of animals.* New York, Dover Publications 1961

[13] **van de Grind W.A. (1990)** *Smart mechanisms for the visual evaluation and control of self-motion*. In: *Warren R & Wertheim A (eds.): Perception and control of self-motion*. Hillsdale NJ, LEA: Ch. 14, 357-398

[14] **Holland J.H. (1975)** *Adaptation in natural and artificial systems*. Univ. Michigan Press

[15] **Holland J.H. and Reitman J.S. (1978)** *Cognitive systems based on adaptive algorithms*. In: *Waterman & Hayes-Roth (eds): Pattern-directed inference systems*. Academic Press

[16] **Holland O and Melhuish C (1996)** *Some adaptive movements of animats with single sensor symmetrical sensors*. In: *Maes P, Mataric M, Meyer J-A, Pollack J and Wilson S.W. (eds): From Animals to Animats 4: Proceeding of the Fourth International Conference on Simulation of Adaptive Behavior*. The MIT Press/Bradford Books, Cambridge, MA.

[17] **Kühn A. (1919)** *Die Orientierung der Tiere im Raum*. Gustav Fischer Verlag, Jena, 1919

[18] **Locket N.A. (1977)** *Adaptations to the deep-sea environment*. In: *Crescitelli F. (ed.): Handbook of Sensory Physiology Vol. VII/5: The visual system in vertebrates*. Berlin/New York, Springer Verlag 1977: Ch.3, 67-192

[19] **Loeb J. (1918)** *Forced movements, tropisms and animal conduct*. Philidelphia, Lippincott 1918; **republished 1973, Dover, New York**

[20] **Lythgoe J.N. (1979)** *The ecology of vision*. Oxford, Clarendon Press, 1979

[21] **Rössler O.E. (1974)** *Adequate locomotion strategies for an abstract organism in an abstract environment-A relational approach to brain function*. In: *Conrad M., Güttinger W. and Dal Cin M. (1974): Lecture Notes in Biomathematics 4: Physics and Mathematics of the Nervous System*. Berlin/New York, Springer Verlag 1974: 342-370

[22] **Schöne H. (1984)** *Spatial orientation. The spatial control of behavior in animals and man*. Princeton N.Y., Princeton University Press 1984

[23] **Terzopoulos D., Tu X., and Grzeszczuk, R. (1994)** *"Artificial Fishes with Autonomous Locomotion, Perception, Behavior, and Learning in a Simulated Physical World*. In: *Brooks R. and Maes P. (eds.): Artificial Life IV: Proc. of the Fourth International Workshop on the Synthesis and Simulation of Living Systems*. Cambridge, MA, 1994: p.17-27

[24] **Walter W.G. (1950)** *An imitation of life*. Scien. Am. 182: 42-45

[25] **Walter W.G. (1951)** *A machine that learns*. Scien. Am. 185: 60-63

[26] **Wilson D.M. and Waldron I. (1968)** *Models for the generation of motor output patterns in flying locusts*. Proc. IEEE 56: 1058-1064

[27] **Wilson D.M. and Weis-Fogh T. (1962)** *Patterned Activity of Co-ordinated Motor Units, studied in flying Locusts*. J. Exp. Biol. 39 1962: 643-667.

[28] **Young H.D. (1992, 8th edition)** *University Physics*. Addison-Wesley Publishing Company, Reading MA 1992

6 Captions and Figures

Figure 1 :

A paddler. The indicated parameters are explained in the text.

Figure 2 :

Retina and visual field of the paddler's eye in polar representation. The receptive fields which make up the retina can, as is indicated, consist of a number of photoreceptors projecting onto a set of ganglion-cells which measure certain local properties of the visual field. In the present paper, the receptive fields consist of only one photoreceptor. Due to the RWF, a Gaussian receptor-sensitivity profile, the response (R1) to a more distant (or smaller) glowball (G1) can be higher than the response (R2) to a closer or larger glowball (G2), if G1 is more "straight ahead" than G2. This is similar to the well-known decrease of resolution with eccentricity.

Figure 3 :

The visuomotor network of the paddler's nervous system. Ⓢ, Ⓧ, ⊜ and ? indicate respectively a summating, a correlating, a threshold and a "random" neurone; τ a leaky integrator neurone, and % a normalising (dividing) neurone. $\rightarrow$ indicates an excitatory synapse, $\dashv$ an inhibitory synapse and —○ a shunting inhibitory synapse. The network is explained in the text.

Figure 4a :

Paths followed in a two-light experiment by a marine amphipod, *Corophium longicorne*,in two equal lights. After [12]

Figure 4b :

Paths followed in a two-light experiment by a paddler without directional selectivity,presented with two identical glowballs. Closed circles represent the glowballs (at (100,65) and (100,35); open circles mark the route-segments where the paddler was eating (= had the glowball in its mouth); diamonds mark the route-segments where the paddler was searching.

Figure 4c :

Paths followed in a two-light experiment by a paddler with directional selectivity,presented with two identical glowballs.

Figure 5 :

Influence of eye-position α and eye axis β on the performance for a low density, $\mathrm{G} = 121$, of large glowballs. For clarity, the $\wp$-axis is reversed.

Figure 6 :

Influence of eye-position α and eye axis β on the performance for a high density, $\mathrm{G} = 625$, of large glowballs.

Figure 7 :

Influence of RWF halfwidth σ on the performance for various glowball populations with large individuals. Error bars indicate the average standard deviation (measured over the performance of 3 paddlers) per curve.

Figure 8 :

Influence of RWF halfwidth σ on the performance for various glowball populations with small individuals. Error bars indicate the average standard deviation per curve.

Figure 9 :

Influence of fixation distance D_f on the performance for $\sigma = 5°$, various eye-positions α and a low glowball density of $\mathrm{G} = 121$. Error bars indicate the average standard deviation per curve.

Figure 10 :
Influence of fixation distance D_f on the performance for $\sigma = 5°$, various eye-positions α and a high glowball density of $\mathrm{G} = 625$. Error bars indicate the average standard deviation per curve.

Figure 11 :
Overview of the forces exerted by a pair of paddles on the paddler-body. F_{rot} is the resultant rotational component of the thrust; F_{trans} the translational component, which works under an angle of σ.

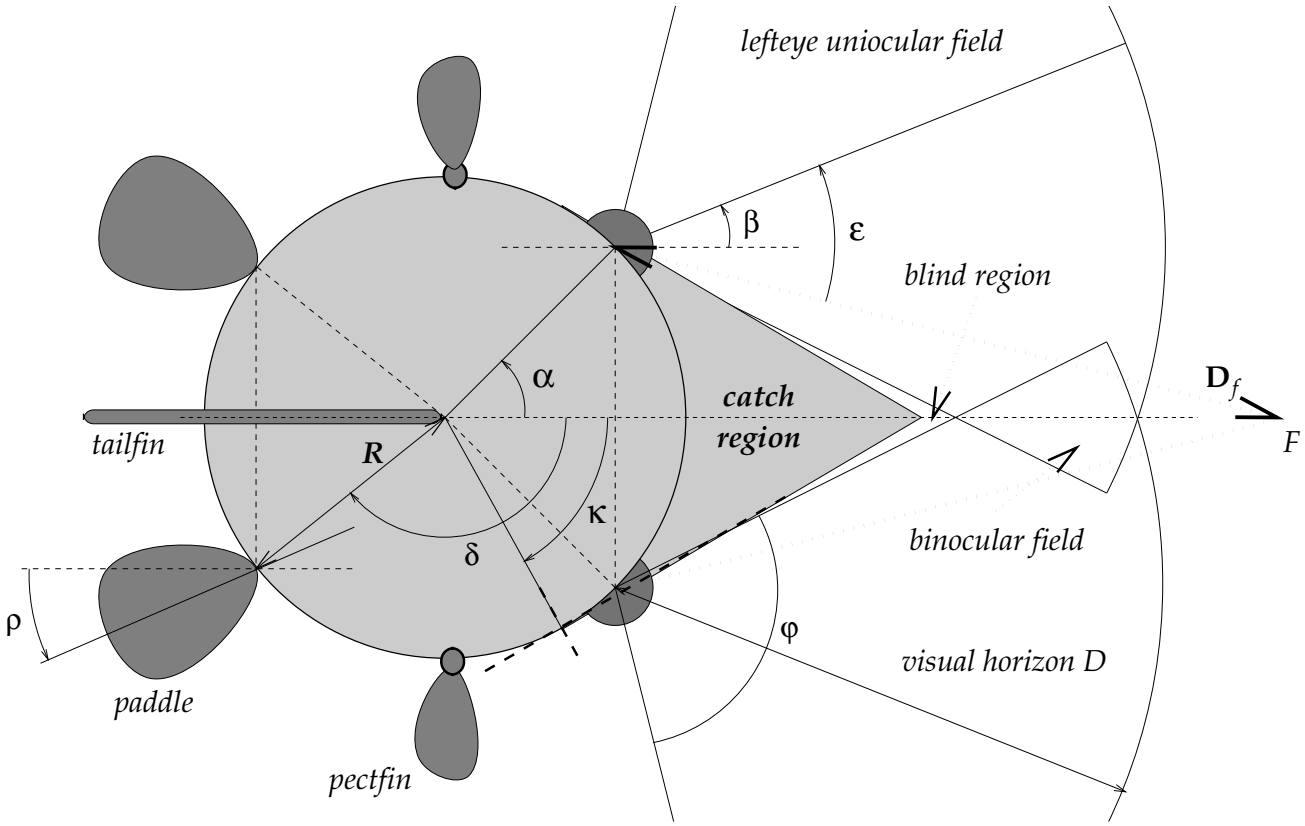
lefteye uniocular field
β
ε
blind region
α
catch
region
D_f
F
tailfin
R
κ
δ
binocular field
ρ
φ
visual horizon D
paddle
pectfin

Figure 1:

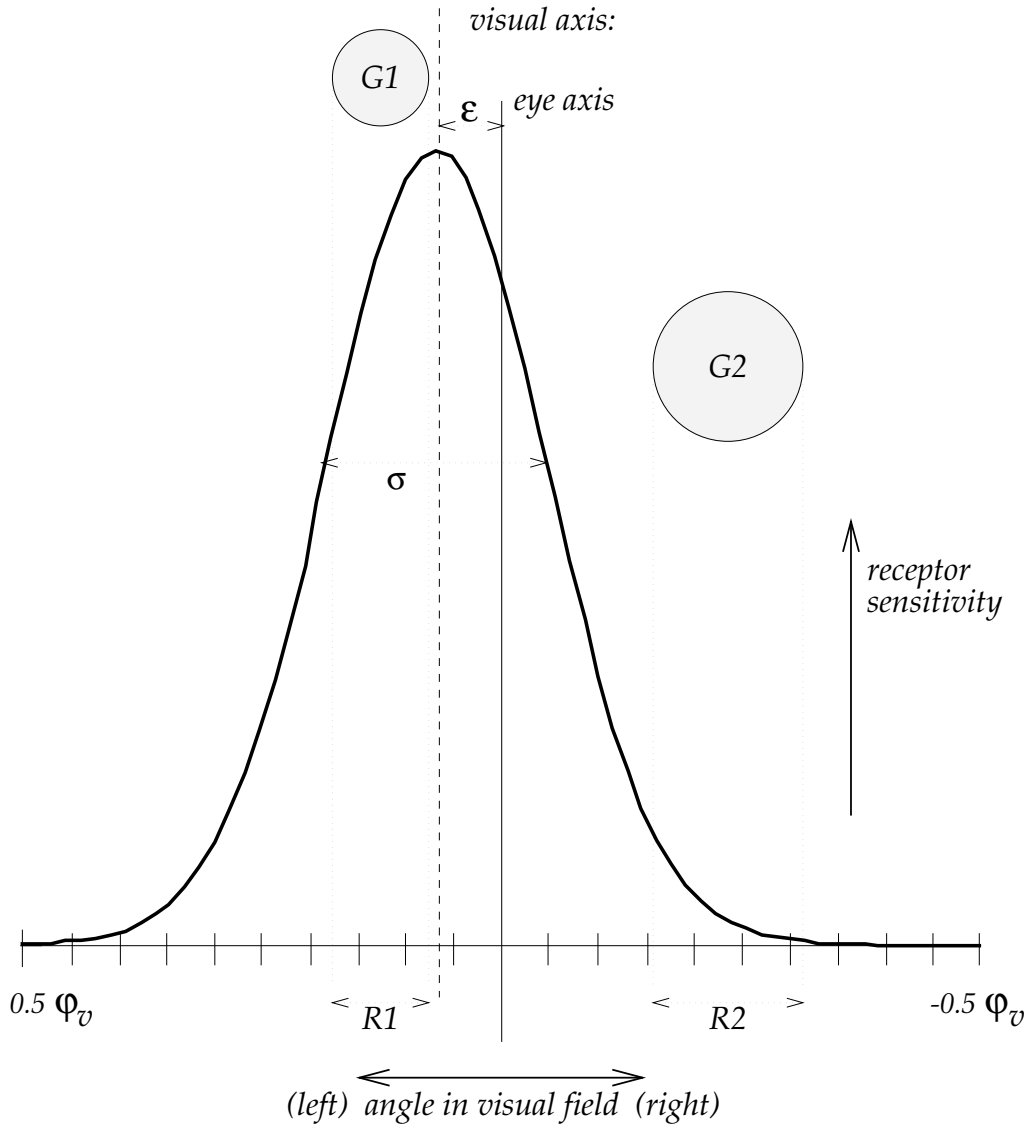
visual axis:
G1
ε
eye axis
G2
σ
receptor
sensitivity
0.5 φv
R1
R2
-0.5 φv
(left) angle in visual field (right)

Figure 2:

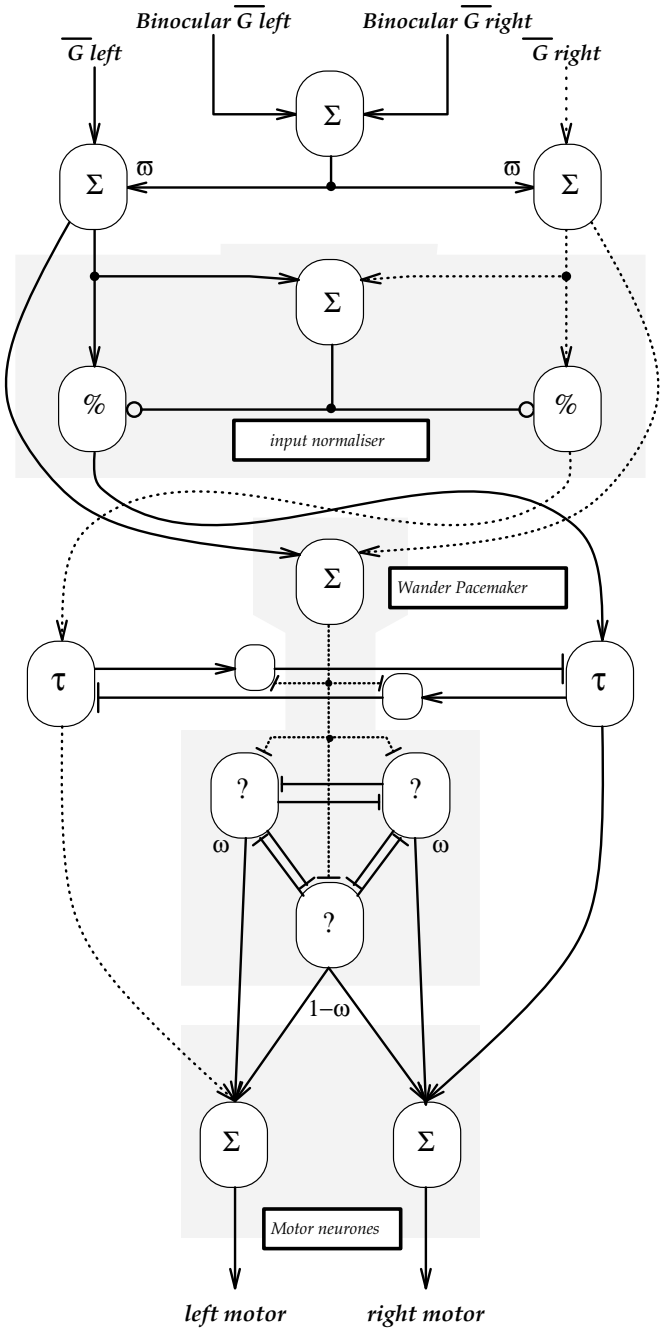
Binocular $\overline{G}$ left
Binocular $\overline{G}$ right
$\overline{G}$ left
$\overline{G}$ right
Σ
ϖ
%
input normaliser
Wander Pacemaker
τ
?
ω
1−ω
Motor neurones
left motor
right motor

Figure 3:

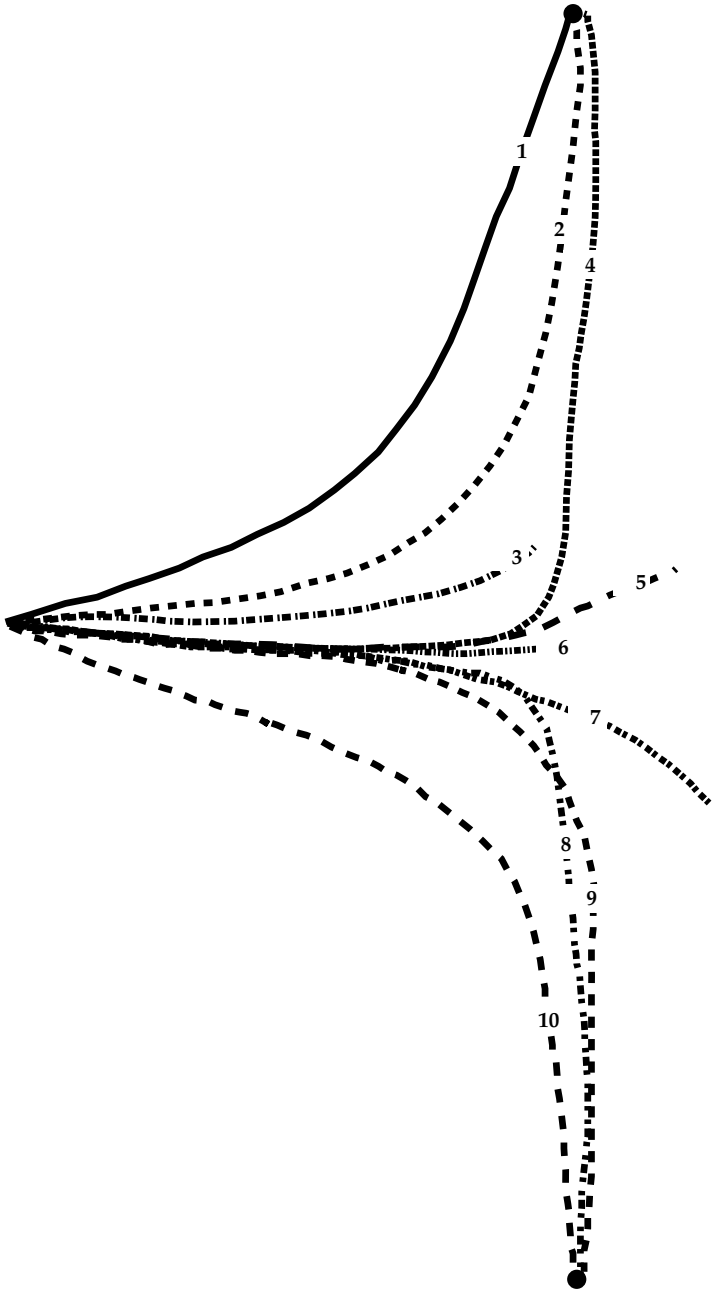

Figure 4:

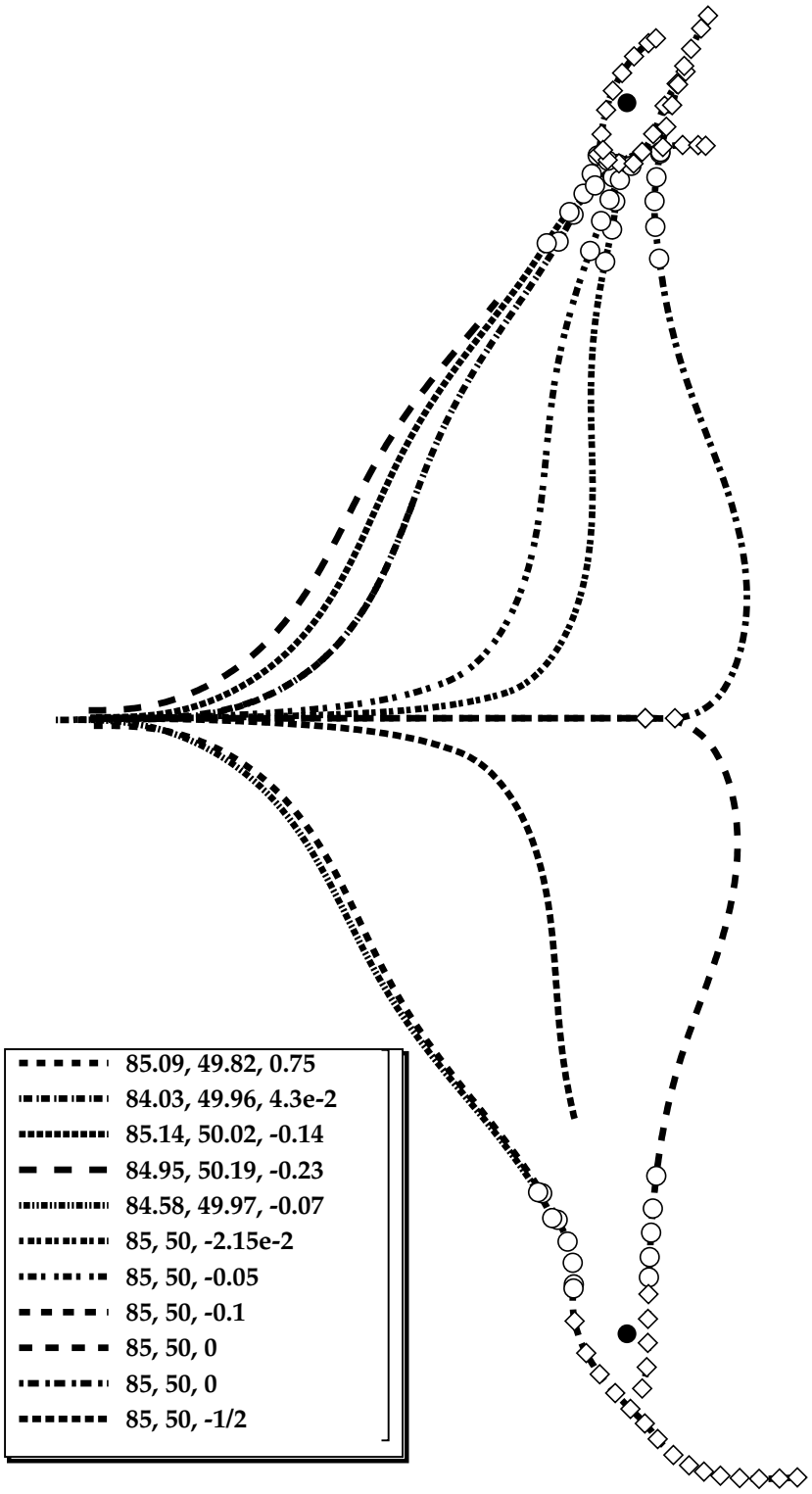
85.09, 49.82, 0.75
84.03, 49.96, 4.3e-2
85.14, 50.02, -0.14
84.95, 50.19, -0.23
84.58, 49.97, -0.07
85, 50, -2.15e-2
85, 50, -0.05
85, 50, -0.1
85, 50, 0
85, 50, 0
85, 50, -1/2

Figure 4b

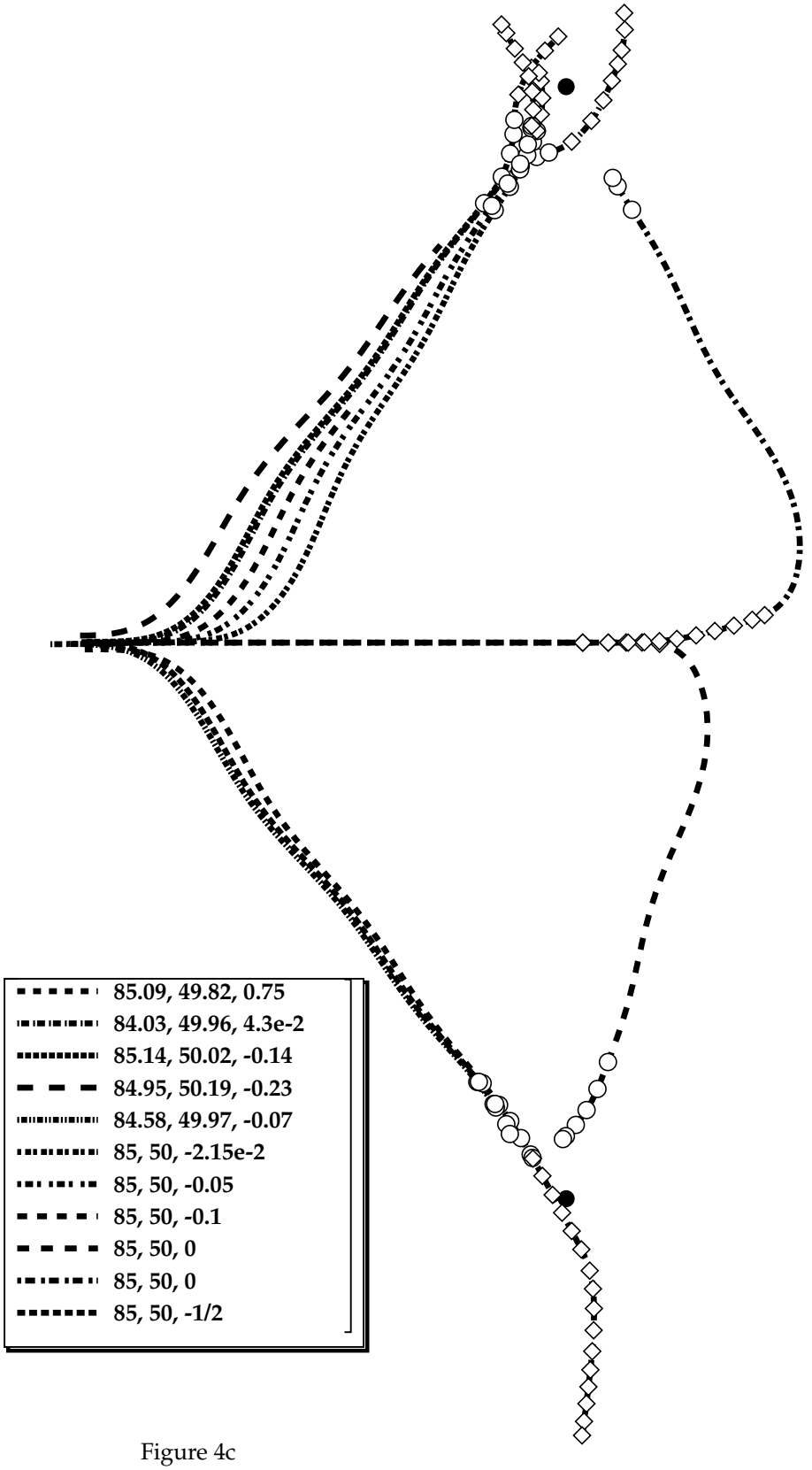
85.09, 49.82, 0.75
84.03, 49.96, 4.3e-2
85.14, 50.02, -0.14
84.95, 50.19, -0.23
84.58, 49.97, -0.07
85, 50, -2.15e-2
85, 50, -0.05
85, 50, -0.1
85, 50, 0
85, 50, 0
85, 50, -1/2

Figure 4c

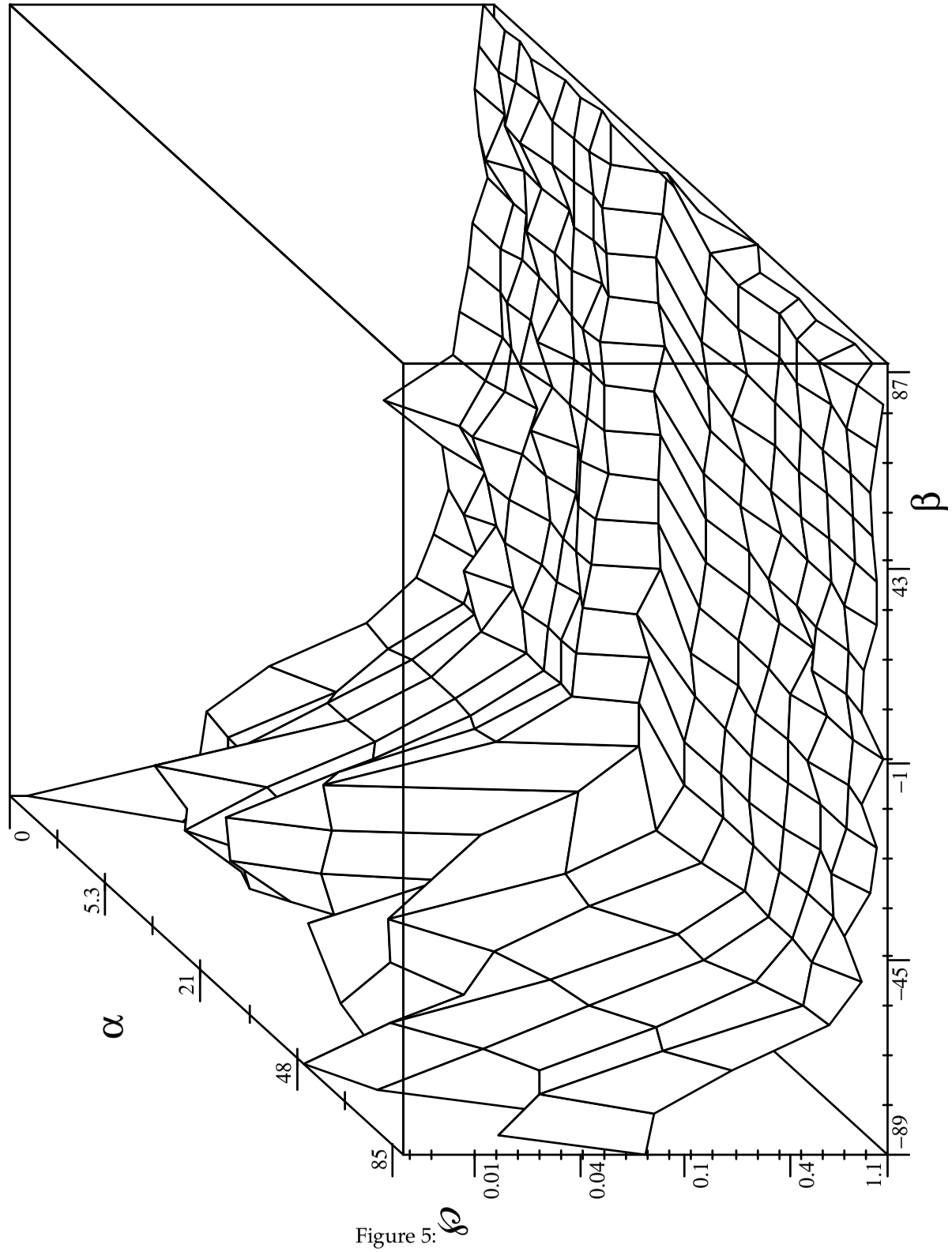

Figure 5:

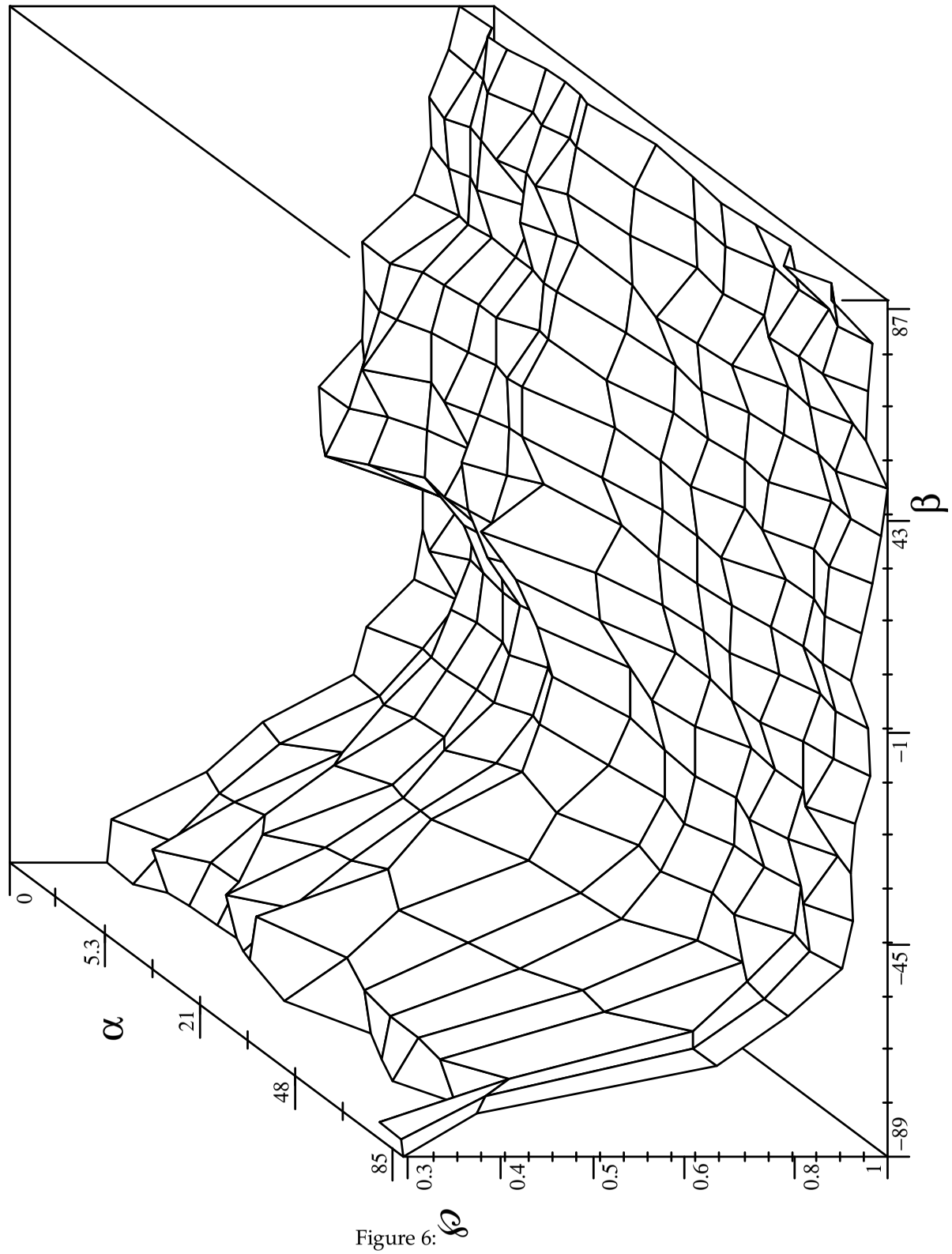

Figure 6:

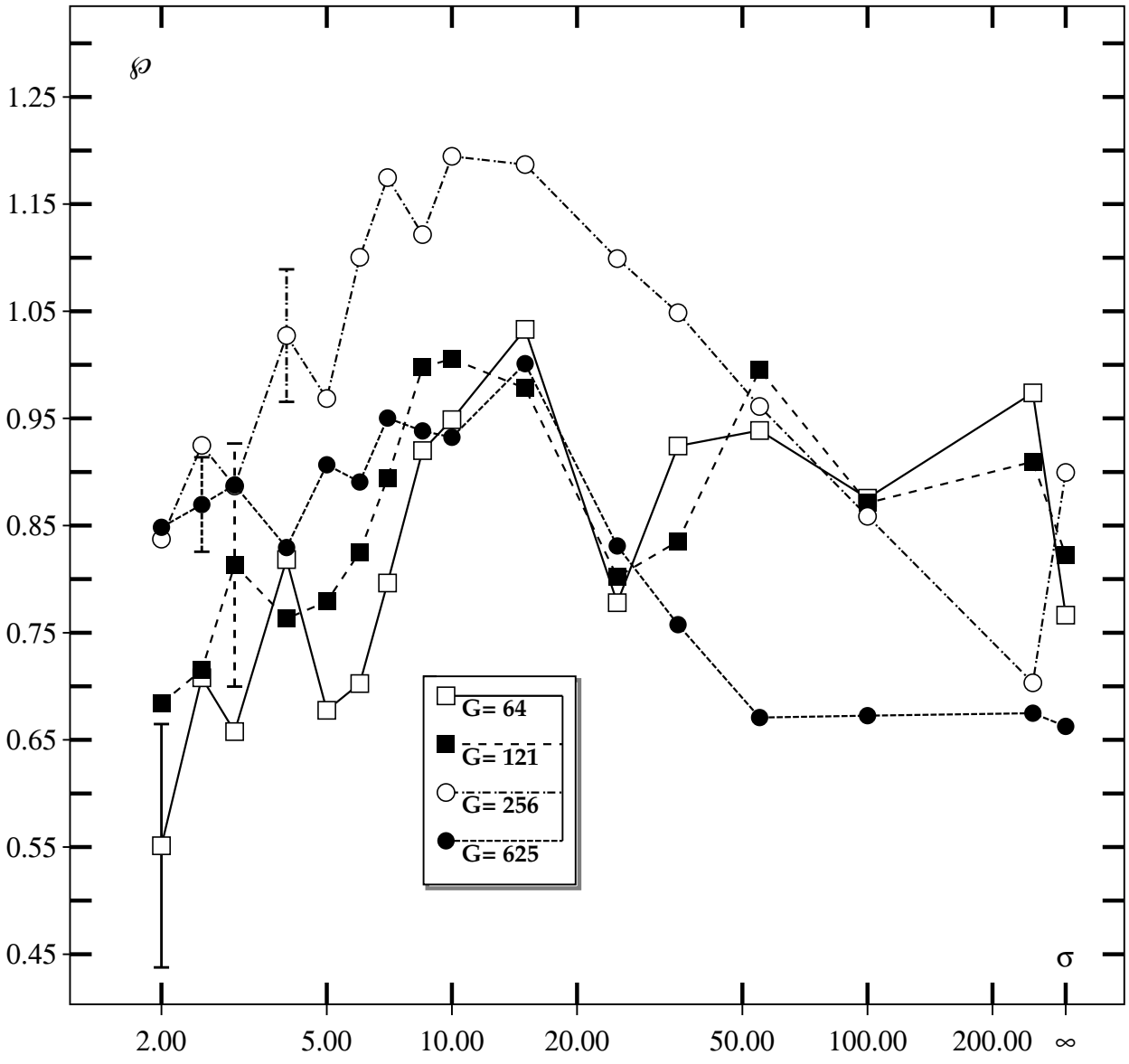
℘
1.25
1.15
1.05
0.95
0.85
0.75
0.65
0.55
0.45
G= 64
G= 121
G= 256
G= 625
σ
2.00
5.00
10.00
20.00
50.00
100.00
200.00
∞

Figure 7:

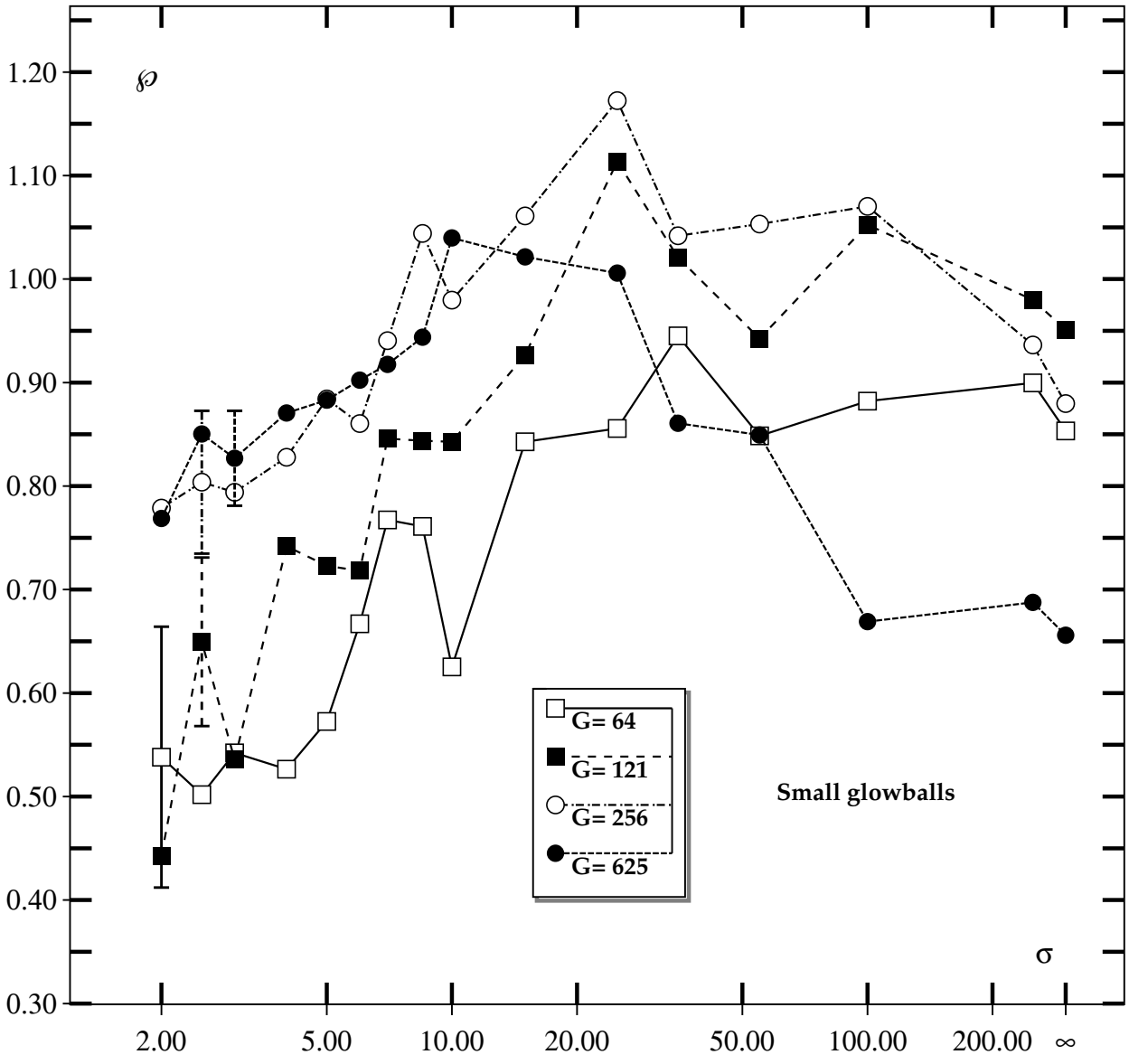
℘
1.20
1.10
1.00
0.90
0.80
0.70
0.60
0.50
0.40
0.30
2.00
5.00
10.00
20.00
50.00
100.00
200.00
∞
σ
G= 64
G= 121
G= 256
G= 625
Small glowballs

Figure 8:

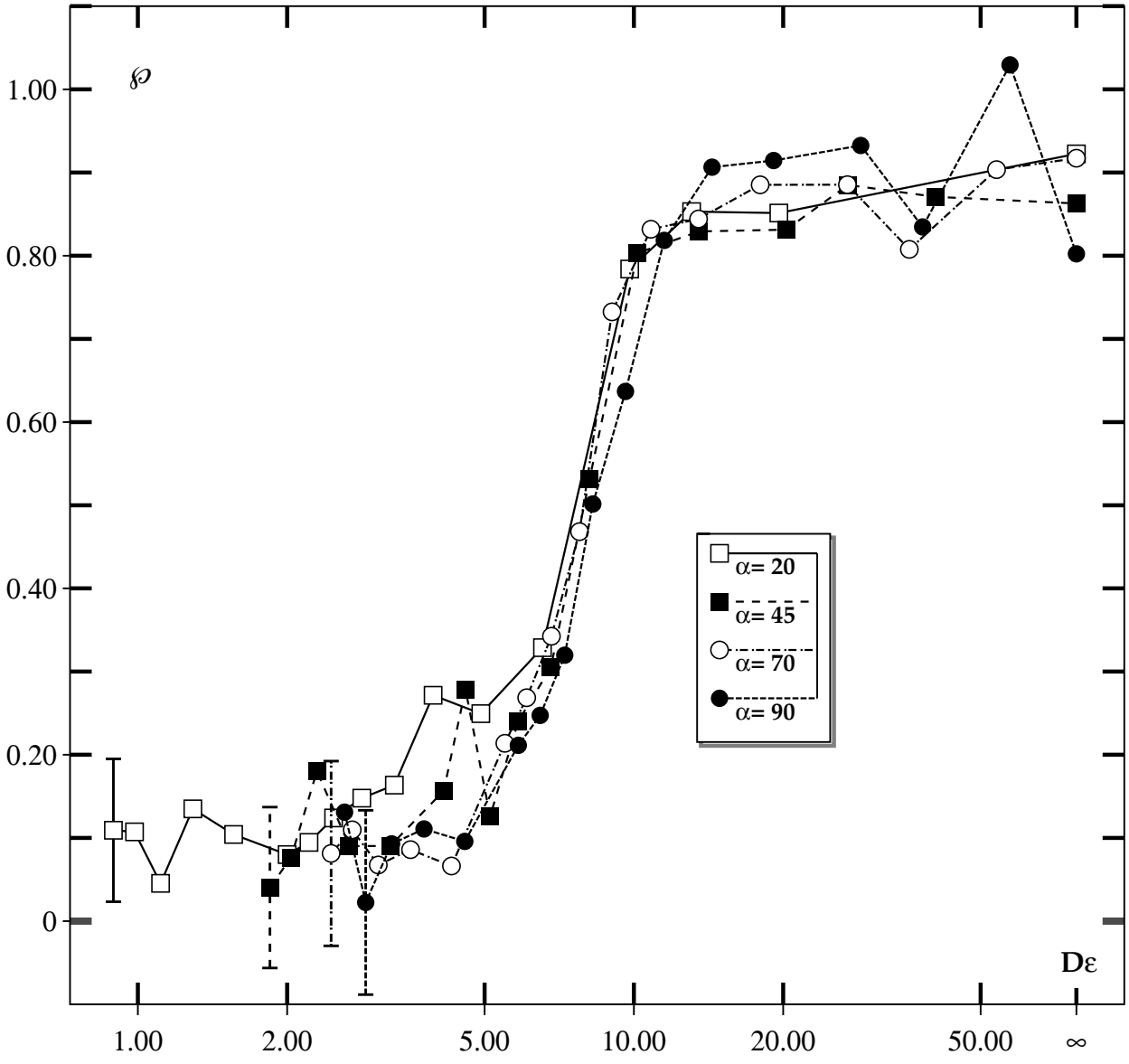
℘
1.00
0.80
0.60
0.40
0.20
0
α= 20
α= 45
α= 70
α= 90
Dε
1.00
2.00
5.00
10.00
20.00
50.00
∞

Figure 9:

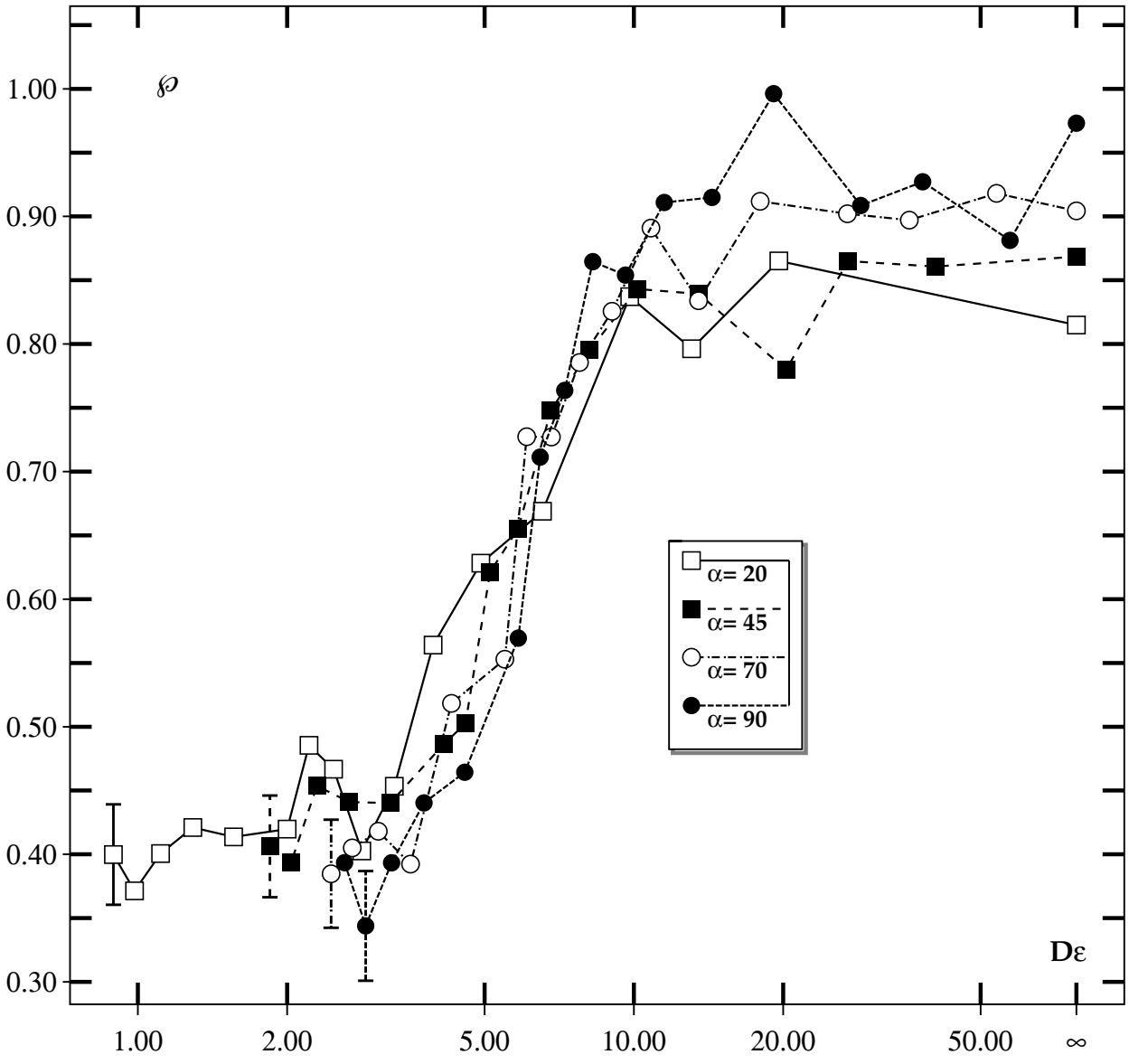
℘
1.00
0.90
0.80
0.70
0.60
0.50
0.40
0.30
1.00
2.00
5.00
10.00
20.00
50.00
∞
Dε
α= 20
α= 45
α= 70
α= 90

Figure 10:

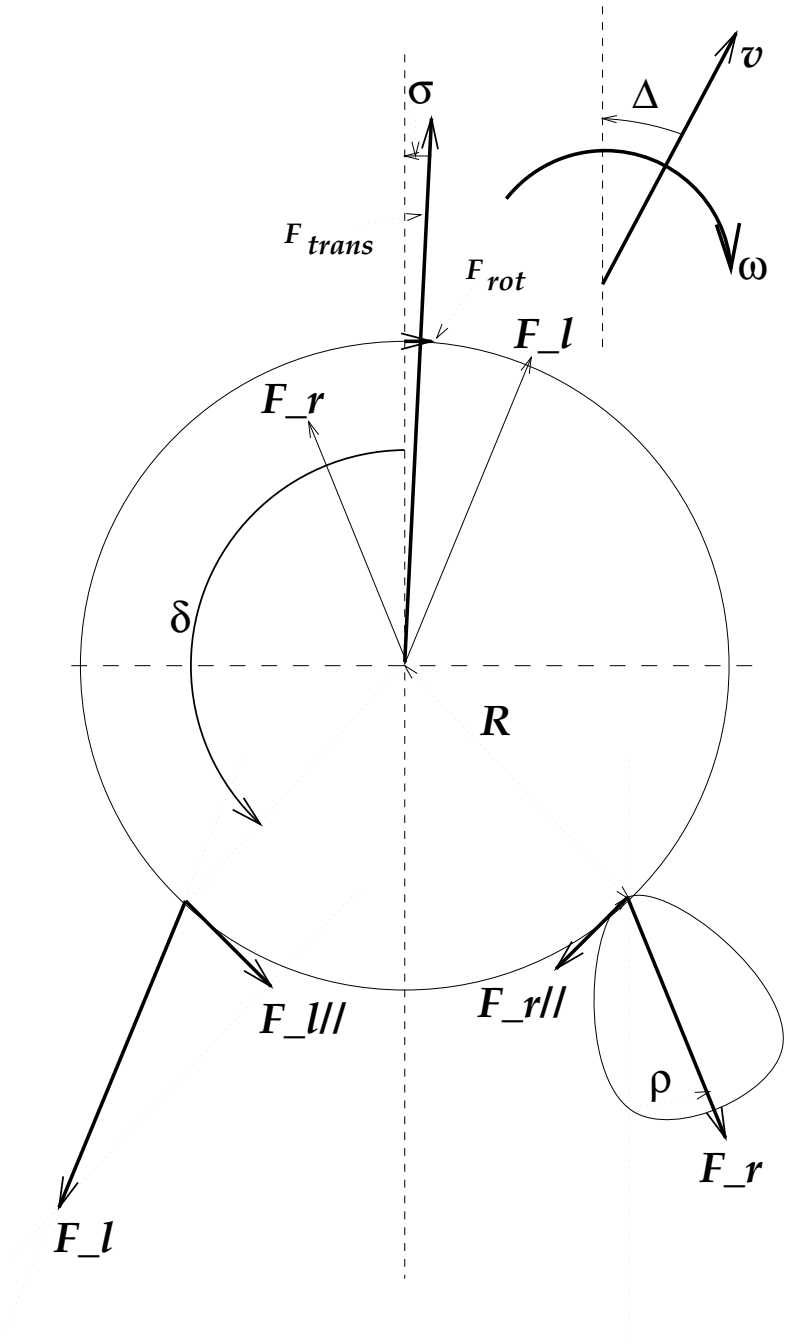

Figure 11: